arXiv:astro-ph/0103341v1 21 Mar 2001

Resonance accretion on the magnetized rotating neutron star

Ya. N. Istomin[1] and A. V. Makarov[2]

[1] P. N. Lebedev Physical Institute, Leninsky Prospect 53, Moscow, 117924 Russia
   e-mail: `istomin@lpi.ru`
[2] Department of General and Applied Physics, Moscow Institute of Physics and Technology,
   Institutsky 9, Dolgoprudny, Moscow region, 141700 Russia
   e-mail: `stalker@dgap.mipt.ru`

Abstract. It is suggested that the accretion disk excites the eigen modes of Alfven oscillations of the magnetic field tubes the ends of which are frozen to the neutron star surface. The resonance takes place when the eigen Alfven frequency coincides with the difference of the Keplerian disk rotation frequency and the frequency of rotation of a neutron star. This model explains the two narrow lines of QPO oscillations in kHz band and permits to calculate the masses and radii of the neutron stars in X-ray binaries.

Key words. Accretion, accretion disks – Waves – Stars: neutron – X-rays: binaries – Stars: individual: Sco X-1

1. Introduction

Rossi X-Ray Timing Explorer (RXTE) in 1996 discovered the quasi-periodic oscillations (QPO) of X-ray emissions in low-mass X-ray binaries (LMXB) in the band of 1 kHz frequencies (van der Klis et al. 1996; van der Klis 2000). They are narrow, the ratio of the line's width to the central frequency can be as low as 10^{-2}, and in most cases there were observed two lines. The existence of such lines means that the accretion disk approaches very close to the surface of the rotating neutron star. Indeed, the Keplerian frequency

$$\nu_{\mathrm{K}} = \frac{1}{2\pi}\left(\frac{MG}{r^3}\right)^{1/2}, \qquad (1)$$

where M is the neutron star's mass and r is the distance from the star's center, is of the order of 1 kHz at the distance of $1.7 \cdot 10^6$ cm for the typical neutron star mass $M \simeq 1.4 \cdot M_\odot$. But estimated neutron star radius R is of about 10^6 cm, and we see that the inner edge of the accretion disk can approach almost to the star surface. If we estimate the kinetic energy of a proton near the star's radius ($r \simeq R$) it turns out of $3 \cdot 10^{-5}$ erg or 20 MeV. For the characteristic proton's density in the accretion flow near the star surface, corresponding to the accretion rate $\dot{M} \simeq 10^{17}$ g/sec ($L_x \simeq L_{\mathrm{Edd}}$), $n_{\mathrm{p}} \simeq 8 \cdot 10^{17}$ cm^{-3}, we obtain the energy density of the accreting plasma of

$$\mathcal{E} \simeq 2.5 \cdot 10^{13} \text{ erg/cm}^3.$$

It seams that for the existence of the disk in the region near the star's surface, the star's magnetic field should not exceed the value of

$$\frac{B^2}{8\pi} < \mathcal{E}, \quad \text{or} \quad B < 2.5 \cdot 10^7 \text{ G.}$$

But this low value of magnetic field on the neutron star surface contradicts with the magnitude of the magnetic field observed for the milliseconds pulsars $B \simeq 10^{9-10}$ G, which are considered originate from the LMXB. But these estimations are incorrect. The plasma destroys the magnetic field structure when its thermal energy exceeds the magnetic field energy, but not when its kinetic flow energy exceeds the magnetic one. Moving across the magnetic field lines plasma polarizes so that the electric field across the magnetic one appears. In the case of a thin disk the radial electric field

$$\boldsymbol{E}_r = -\frac{1}{c}[\boldsymbol{v}_{\mathrm{K}}\boldsymbol{B}] \qquad (2)$$

is enough to carry the flow across the magnetic field with the Keplerian velocity $v_{\mathrm{K}} = 2\pi\nu_{\mathrm{K}}r$. For the dipole magnetic field ($B \propto r^{-3}$) the disk of the temperature T destroys the star's magnetic field at the distances

$$r > r_A = R\left[\frac{B^2 R^2}{4\dot{M}(T/m_{\mathrm{p}})^{1/2}}\right]^{1/4} \qquad (3)$$

If we substitute to (3), the characteristic energy of X-ray emission (~ 1 keV) as the maximum disk temperature we
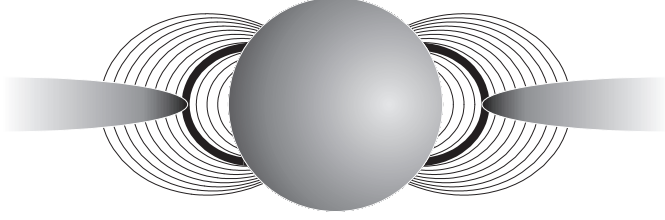
Fig. 1. The accreting disk approaches so close to the neutron star surface, that plasma flow along the magnetic field lines.

obtain

$$r > 20R \left(\frac{B}{10^9 \text{ G}} \right)^{1/2}.$$

Thus, we see that in the region where QPO of 1 kHz frequency can originate the structure of the magnetic field of the star is not disturbed by the accreting plasma. We can consider that the structure of the magnetic field near the star surface($r \leq 10R$) is given by the interior of the neutron star and has the dipole configuration. Besides, the accretion changes the initial neutron star magnetic field $B \simeq 10^{12}$ G up to $B \simeq 10^9$ G. And it is naturally to consider the direction of the dipole magnetic momentum $\boldsymbol{\mu}$ coinciding with the axis of star's rotation $\boldsymbol{\Omega}$.

We assume that the accreting disk approaches close to the neutron star surface. Plasma flows from the disk to the neutron star along magnetic field lines and form so-called "magnetic field plasma tubes", which are shaped as magnetic field lines, are filled with plasma and have a small thickness.

The narrow structure of the QPO of 1 kHz frequency suggests the resonance nature of its origin. We have the idea that it is a resonance between Keplerian rotation of the disk and an eigen modes of the oscillation of magnetic field tubes, frozen to the conducting star surface.

Such model is more close to the sonic point beat frequency model (Miller et al. 1998), where the resonance takes place not with the Keplerian rotation of the disk, but with the radial motion of accreting flow coinciding with the sonic velocity. The other model based on the eigen modes of the disk in the rotating frame was proposed by Titarchuk & Osherovich (1999). There is more exotic mechanism proposed by Klein et al. (1998) where QPOs are the oscillations of photon's bubbles.

2. Magnetic tubes oscillations

In this section we discuss the oscillations of the magnetic field lines with plasma frozen to them. Discovering this model it is convenient to use the dipole coordinates (l, a) introduced by the definition:

$$\boldsymbol{B} = -\boldsymbol{\nabla} l;$$
$$\boldsymbol{B} = [\boldsymbol{\nabla} a, \boldsymbol{\nabla} \phi]. \tag{4}$$

l is the coordinate along the magnetic field line

$$l = \frac{(\boldsymbol{\mu r})}{r^3} = \mu \frac{z}{(\varrho^2 + z^2)^{3/2}}, \tag{5}$$

a numerates the magnetic field surfaces

$$a = \mu \frac{\varrho^2}{(\varrho^2 + z^2)^{3/2}}. \tag{6}$$

$a = \text{const}$ is the equation for the magnetic field lines

$$z^2 = (\frac{\mu}{a})^{2/3} \varrho^{4/3} - \varrho^2, \quad \text{or} \quad r = \frac{\mu}{a} \sin^2 \theta. \tag{7}$$

Here (ϱ, z) are the cylindrical coordinates, (r, θ) are the spherical ones. The value of a is also connected with the maximum deflection ϱ_{max} of the dipole magnetic field line from the star's center $a = \mu/\varrho_{max}$. For different magnetic surfaces the coordinate a changes from 0 to μ/R. The coordinate l changes for a given a, from $-(\mu^2 - \mu Ra)^{1/2}/R^2$ to $(\mu^2 - \mu Ra)^{1/2}/R^2$. The point $l = 0$ corresponds to the top of the magnetic field line. Three coordinates (l, a, ϕ) (ϕ is the azimuthal angle) are the curvilinear orthogonal coordinate system.

Because in the near $(r < 10R)$ region $B^2/8\pi \gg \mathcal{E}$ the plasma can be considered as cold, the plasma density is proportional to the magnetic field strength, $n_{\text{p}} = \lambda B$. Here λ is the constant not depending on the coordinates. The equations of the ideal MHD in rotating with angular velocity Ω frame (Ω is the star rotation frequency) can be presented for the electric current $\boldsymbol{j}$ as follows

$$\boldsymbol{j} = \frac{v_A^2}{\omega^2 B} \text{rot rot} \left\{ \frac{1}{B} \Big[\boldsymbol{B}[\boldsymbol{jB}] \Big] \right\}, \tag{8}$$

where v_A is the Alfven velocity

$$v_A^2 = B^2/4\pi n_{\text{p}} m_{\text{p}} = B/4\pi \lambda m_{\text{p}}.$$

We consider here that all the perturbed values $\boldsymbol{j}$, $\delta \boldsymbol{B}$, $\boldsymbol{E}$ depend on the time t and the azimuthal angle ϕ as $\exp\{-i\omega t + im\phi\}$.

The electric current can be presented through its co-variant components j_1, j_2, j_3

$$\boldsymbol{j} = j_1 \boldsymbol{\nabla} l + j_2 \boldsymbol{\nabla} a + j_3 \boldsymbol{\nabla} \phi,$$

for which from (8) we obtain

$$j_2 \left(1 - \frac{v_A^2}{\omega^2 \varrho^2} m^2 \right) + \frac{v_A^2}{\omega^2 \varrho^2 B} \frac{\partial}{\partial l} \left[\varrho^2 B^2 \frac{\partial}{\partial l} (j_2 B) \right] =$$
$$im \frac{v_A^2}{\omega^2 \varrho^2 B} \frac{\partial}{\partial a} (j_3 B); \tag{9}$$

$$j_3 + \frac{v_A^2 \varrho^2 B}{\omega^2} \left[\frac{\partial^2}{\partial a^2} (j_3 B) + \frac{\partial}{\partial l} \frac{1}{\varrho^2} \frac{\partial}{\partial l} (j_3 B) \right] =$$
$$im \frac{v_A^2 \varrho^2 B}{\omega^2} \frac{\partial}{\partial a} (j_2 B); \tag{10}$$

$$j_1 = \frac{v_A^2}{\omega^2 B} \left[\frac{\partial}{\partial a} \varrho^2 B^2 \frac{\partial}{\partial l} (j_2 B) + \frac{im}{\varrho^2} \frac{\partial}{\partial l} (j_3 B) \right]. \tag{11}$$

The boundary conditions for (9, 10, 11) are on the star surface $r = R$. Due to the ideal conductivity of neutron star matter the tangential components of the electric field have to be zero. The electric field of the disturbance is proportional to the electric current

$$\boldsymbol{E} = \frac{iB}{\omega c^2 \lambda} \left(j_2 \, \boldsymbol{\nabla} \, a + j_3 \, \boldsymbol{\nabla} \, \phi \right).$$

It gives the boundary conditions for j_2 and j_3

$j_2 = j_3 = 0$ at $r = R$, or

$$l = \pm l_m = \pm \left(\mu^2 - \mu R a \right)^{1/2} / R^2. \quad (12)$$

Equation (9) describes the Alfven type oscillations because it contains only the second derivatives over longitudinal coordinate l, but equation (10) is that for the magnetosonic waves (also the derivatives over a coordinate). In the case of nonaxial symmetric oscillations ($m \neq 0$) these modes are coupled. We consider the case when the accretion disk excites the MHD waves in the magnetosphere with the dipole magnetic field. Rotating with the Keplerian frequency ω_K different from the star rotation frequency Ω, the conducting disk deflects the magnetic field lines in equatorial plane to ϕ-direction. Because this deflection is symmetric over ϕ we consider here only the case $m = 0$. As Alfven and magnetosonic oscillations are independent and Alfven wave has only the ϕ component of the disturbed magnetic field

$$j_2 = -\frac{c}{4\pi \varrho^2} \frac{\partial \delta B_3}{\partial l},$$
$$\delta \boldsymbol{B} = \delta B_1 \, \boldsymbol{\nabla} \, l + \delta B_2 \, \boldsymbol{\nabla} \, a + \delta B_3 \, \boldsymbol{\nabla} \, \phi, \quad \delta B_3 = \varrho \cdot \delta B_\phi,$$

while the magnetosonic has two, δB_1 and δB_2

$$j_3 = \frac{cB^2 \varrho^2}{4\pi} \left(\frac{\partial \delta B_2}{\partial l} - \frac{\partial \delta B_1}{\partial a} \right). \quad (13)$$

For this reason we choose only the Alfven wave ($\delta B_1 = \delta B_2 = 0$, $\delta B_\phi \neq 0$)

$$j_2 + \frac{v_A^2}{\omega^2 \varrho^2 B} \frac{\partial}{\partial l} \left[\varrho^2 B^2 \frac{\partial}{\partial l} \left(j_2 B \right) \right] = 0. \quad (14)$$

The boundary conditions

$$j_2 \left(a, \, l = \pm l_m \right) = 0$$

imply the quantization of eigen frequencies of the Alfven modes

$$\omega = \omega_j(a), \quad j = 1, 2, \dots$$

After parameterization the eigen frequencies can be presented in the form

$$\omega_j = \omega_0 \cdot \omega_j'(f), \quad (15)$$

where

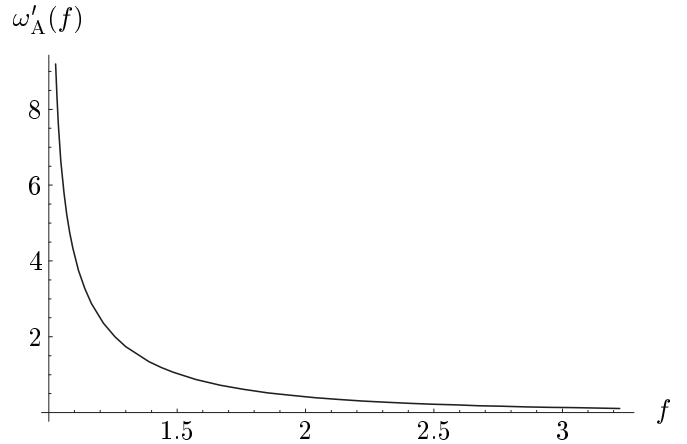$$\omega_0 = \left(\frac{\mu}{4\pi R^5 \lambda m_p} \right)^{1/2},$$

Fig. 2. The dependence of Alfven first harmonics ω_A' on f.

is the characteristic Alfven frequency, and ω_j' is the dimensionless amplitude depending on the dimensionless parameter $f = \varrho_{\max}/R$, which means the height of the dipole magnetic field line in the star radius units. The calculation for the general mode $j = 1$ gives the dependence of on f as pictured on Fig. 2. At large f the eigen frequency falls down like $\omega_A' \propto f^{-5/2}$. The reason of this behavior is that the main contribution to the frequency gives the wave structure in the top of magnetic field tube. Indeed, multiplying the (14) on to $\left(B^2 \varrho^2 \omega^2 / v_A^2 \right) \cdot j_2^*$ and integrating it over l from $-l_m$ to $+l_m$, we get

$$\omega^2 = \frac{\int_{-l_m}^{l_m} \varrho^2 \left| B \frac{\partial}{\partial l} \left(B j_2 \right) \right|^2 \mathrm{d}l}{\int_{-l_m}^{l_m} \frac{\varrho^2}{v_A^2} \left| \left(B j_2 \right) \right|^2 \mathrm{d}l}. \quad (16)$$

From (16) it is seen that $\omega \simeq \left(v_A \right)_{\min} / L$, where L is the length of the magnetic field line. Because of $v_A = \left(B/4\pi \lambda m_p \right)^{1/2} \propto f^{-3/2}$ and $L \propto f$ we obtain the calculated dependence

$$\omega \propto f^{-5/2} \quad (f \gg 1).$$

As for the values of f near the star surface $|f-1| \ll 1$, then $L \propto (f-1)^{1/2}$ and $\omega \propto (f-1)^{-1/2}$ ($f \simeq 1$) as imagined on the Fig. 2. For the same reason the more high modes have the frequencies very close to the harmonics of the general mode

$$\omega_j \simeq j \cdot \omega_1, \quad \omega_A \equiv \omega_1. \quad (17)$$

For the plasma density of $n_p \simeq 8 \cdot 10^{17}$ cm^{-3} near the star surface and magnetic momentum $\mu \simeq 10^{27}$ G·cm^3 ($B \simeq 10^9$ G) the frequency ω_A is of the order of 2π kHz at the distance $r \simeq 5.6R$. It means that QPO of 1 kHz can appear as the result of the resonance of the disk rotation and Alfven eigen modes excited by the disk

$$i \cdot \left(\omega_K - \Omega \right) = \omega_j \simeq j \cdot \omega_A. \quad (18)$$

Here i is the integer number. The resonance condition (18) defines the magnetic field tubes, where the resonance occur, $f_{i,j}$:

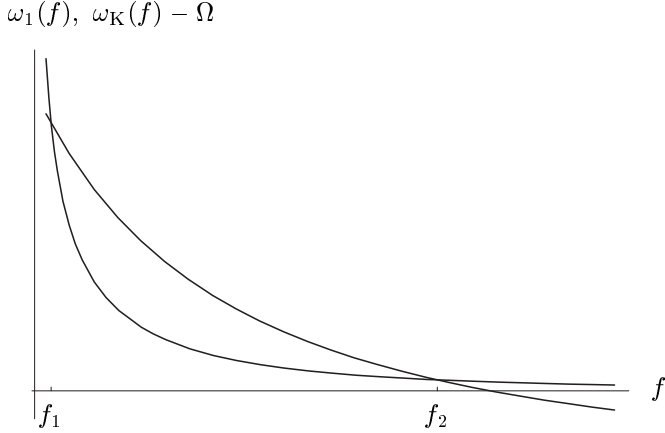$$\omega_K(f_{i,j}) - \Omega = \frac{j}{i} \omega_A(f_{i,j}). \quad (19)$$

$\omega_1(f),\ \omega_{\mathrm{K}}(f) - \Omega$

Fig. 3. There are two general solutions f_1 and f_2 of the (18).

$\omega_{\mathrm{s}}'(f)$

Fig. 4. The dependence of sonic first harmonics ω_{s}' on f.

The solution of (18) is pictured on the Fig. 3. In general case we have two solutions f_1 and f_2 $(f_2 > f_1)$. Their positions are not constants in time because of the changing of the accretion rate and as a consequence of changing of the plasma density n_{p}. The frequency of the Alfven eigen modes $\omega_j \propto n_{\mathrm{p}}^{-1/2}$. It means that higher accretion rate (or n_{p}) larger f_1 and smaller f_2. Accordingly $\omega_{\mathrm{K}}(f_1)$ becomes larger, but $\omega_{\mathrm{K}}(f_2)$ becomes smaller. The observed changes of QPO frequency correspond to the behavior of the root f_1. Apart, it is observed the clear proportionality between intensity of X-ray emission and the frequency of QPO of 1 kHz band. We consider that the resonance at $f = f_1$ is more strong than at $f = f_2$ because of

- it is more close to the star surface where the dipole magnetic field is large; and
- usually f_2 is large enough, so that $\omega_{\mathrm{K}}(f_2)$ falls down from the 1 kHz frequencies.

Further we will discuss only the high frequency solution $f = f_1$. How the QPO frequencies are connected with discussed resonance? At first the excited Alfven oscillations will destroy the accretion disk. The magnetic field gives the drift velocity δv_z for the disk plasma particles

$$\delta \boldsymbol{v}_z = c\frac{[\boldsymbol{E}_r\,\delta\boldsymbol{B}_\phi]}{B^2}; \quad \mid \delta v_z \mid = v_{\mathrm{K}}\frac{\delta B_\phi}{B}, \tag{20}$$

(see $\boldsymbol{E}_r$ from (2)). The disk matter will be pushed from equatorial plane in the direction along the dipole magnetic line to the star surface. And the accretion flow will be modulated by the frequency $\omega_j(f_1) + \Omega$. The point $f = f_1$ will be factually the inner edge of the accretion disk. In observed X-ray emission we can see several characteristic frequencies:

1. $\omega_{\mathrm{K}}(f_1)$, it is the modulation of the X-ray flux by the inhomogeneity of the inner edge of the disk;
2. $\omega_{\mathrm{K}}(f_1) - \Omega$, it is the beating frequency corresponding to the scattering of X-rays from the sources on the star surface, rotating with Ω, by the inner edge of the disk;
3. $\omega_j(f_1) + \Omega = i \cdot \omega_{\mathrm{K}}(f_1) + (1 - i) \cdot \Omega$, it is the frequency of the accretion flow modulated by Alfven oscillations;
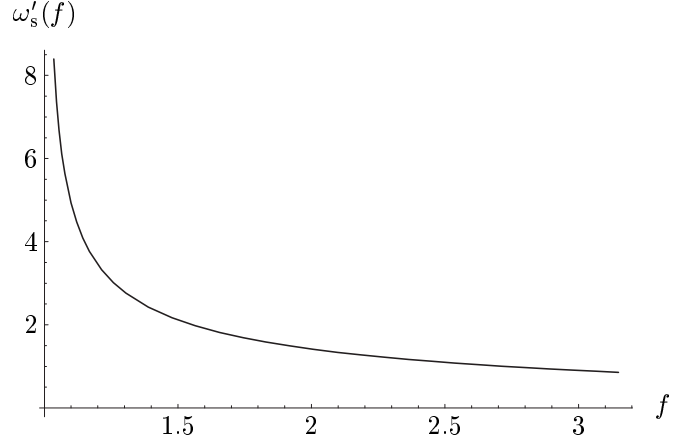
4. different combinations of frequencies 1, 2, 3.

3. Sonic oscillation

It is naturally to consider that the plasma flow along the tube $f = f_1$ is not stationary. The sound mode can be excited.

Let us consider plasma as isothermic with temperature T. For disturbance of concentration δn along the magnetic tube we receive from hydrodynamics

$$\delta n + \frac{T}{m_{\mathrm{p}}\omega^2}\,\mathrm{div\,grad}\,\delta n = 0. \tag{21}$$

In dipole coordinates it looks like

$$\delta n + \frac{T}{m_{\mathrm{p}}\omega^2}B^2\frac{\partial^2}{\partial l^2}\delta n = 0. \tag{22}$$

The boundary condition is on the star surface. The plasma velocity component which is normal to the surface must be equal to zero.

$$\boldsymbol{v} = -\,i\frac{T}{m_{\mathrm{p}}n_{\mathrm{p}}\omega}\,\boldsymbol{\nabla}\,\delta n\bigg|_{l=\pm l_m} = 0. \tag{23}$$

The first harmonics corresponding to the solution of this equation with boundary condition can be presented as

$$\omega(f) = \omega_{\mathrm{s}} \cdot \omega_{\mathrm{s}}'(f), \tag{24}$$

where $\omega_{\mathrm{s}}^2 = T/m_{\mathrm{p}}R^2$ and $\omega_{\mathrm{s}}'(f)$ is dimensionless function on f, which is presented on the Fig. 4, $\omega_{\mathrm{s}}'(f)$ is of the order of 1 when $f \sim 2$. In the region of $f \approx 1$ the function $\omega_{\mathrm{s}}'(f)$ can be approximated by the expression $2/(\pi\sqrt{f - 1})$. So, ω_0 is the charachteristic frequency for sonic oscillation. If we take $T = 1$ keV and $R = 10$ km then $\omega_0 = 30$ s^{-1} or $\nu_0 = 4.9$ Hz. Thus, sonic oscillation can be found on 10 Hz band that is observed simaltaneously with the QPO of 1 kHz band.
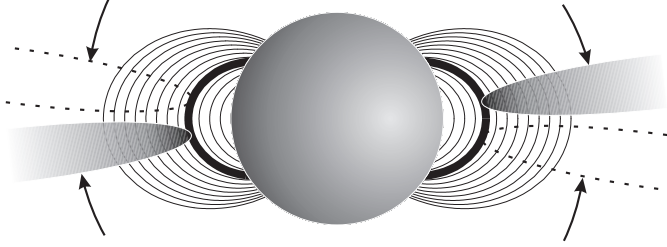
Fig. 5. Due to Kerr metrics the disk precesses with Lense-Thirring frequency.

4. Lense-Thirring precession

While the accreting disk is spinning at the distance r about the neutron star with Keplerian frequency, it precesses about its equilibrium position with Lense-Thirring frequency due to Kerr metrics (Thorne et al. 1986; Morsink & Stella 1999)

$$\omega_{\text{LT}} = a \frac{r_g}{r^3 + (a/c)^2 (r_g + r)}, \qquad (25)$$

where $a = J/M$ ($J = I\Omega$ is the star's angular momentum and $I = 2MR^2/7$ is the momentum if inertia of the star), $r_g = 2GM/c^2$ is the gravitational radius of the neutron star of mass M and radius R.

In the system of units where M is measured in masses of sun and R in 10 km the Lense-Thirring frequency can be presented in the form of

$$\omega_{\text{LT}} = 8.44 \cdot 10^{-2} \, \frac{M\Omega}{R} f^{-3}. \qquad (26)$$

For $M/R \simeq 1$, $f \simeq 1$ and $\Omega \simeq 2\pi \cdot 300 \text{ s}^{-1}$ ω is of the order of $2\pi \cdot 25 \text{ s}^{-1}$. The second harmonics of Lense-Thirring precession is usually observed (Stella & Vietri 1999). In our model it can be illustrated by the fact that some mass is thrown out the disk each time it is in extreme position, i.e. with frequency $2\omega_{\text{LT}}$ (see Fig. 5).

5. Scorpius X-1

We have applied our speculations for Sco X-1 (van der Klis et al. 1996). There were observed 4 QPOs: 6–20 Hz normal/flaring quasi-periodic oscillations; 45 Hz QPOs and two kHz QPOs. According to our model we ascribed the 6–20 Hz QPOs to the sound oscillations, 45 Hz QPOs to Lense-Thirring oscillations, and two kHz QPOs to Alfven and Keplerian oscillations correspondingly.

Below we use the system of units where temperature is measured in eV, masses of objects – in masses of sun and distances – in 10 km. Thus, we can write

$$\text{for sonic:} \quad \omega_{\text{s}}(f) = 0.98 \sqrt{\frac{T}{R^2}} \, \omega_{\text{s}}'(f), \qquad (27)$$

$$\text{for Keplerian:} \quad \omega_{\text{K}}(f) = 11.5 \cdot 10^3 \sqrt{\frac{M}{R^3}} \, f^{-3/2}, \quad (28)$$

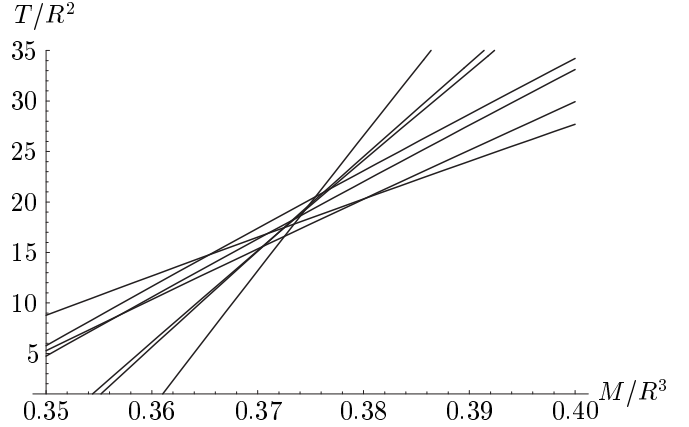where $f = r/R$ – a parameter that characterizes the distance between the disk and neutron star surface.

Fig. 6. Each line on this graph corresponds to one measurment of sonic and Keplerian frequencies. T is measured in eV, M in $M_\odot$, R in 10 km.
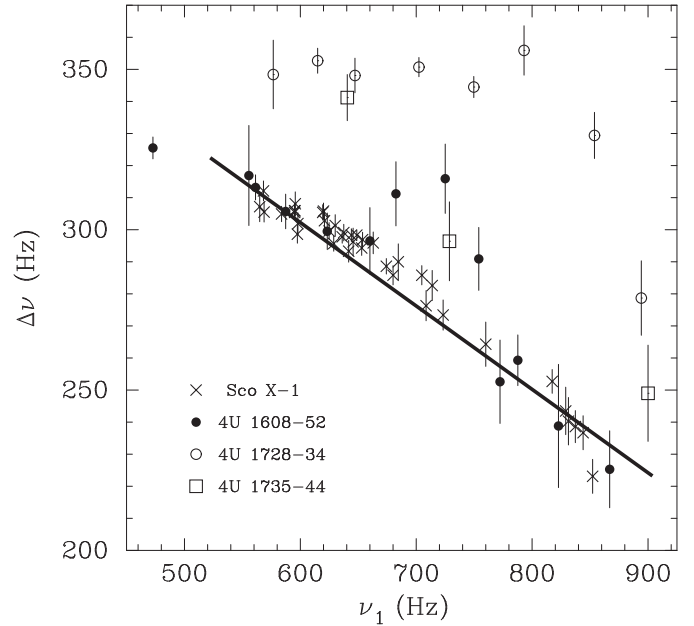

Fig. 7. The variations in kHz QPO peak separation as a function of the lower kHz frequency (Méndez & van der Klis 1999). It is well-seen that for Sco X-1 the dependence is linear.

For every pair of data $(\omega_{\text{K}}, \omega_{\text{s}})$ we can build a curve in $\left(\frac{M}{R^3}; \frac{T}{R^2}\right)$ space. This results in the graph on Fig. 6.

The axis of abscissae is the space for possible meanings of the ratio of M/R^3. For each of possible meanings of this ratio we can find the temperature T (or, to be more accurate, the ratio T/R^2) for each experiment on determining the frequencies ω_{K} and ω_{s}. So we can evaluate the range of the change of temperature T. One can find it remarkable that all the curves cross each other in almost one point! So we can suppose that the temperature of the disk is approximately constant. From the graph we determine $M/R^3 = 0.374 \pm 0.004$ and $T/R^2 = 16.8 \pm 0.8$.
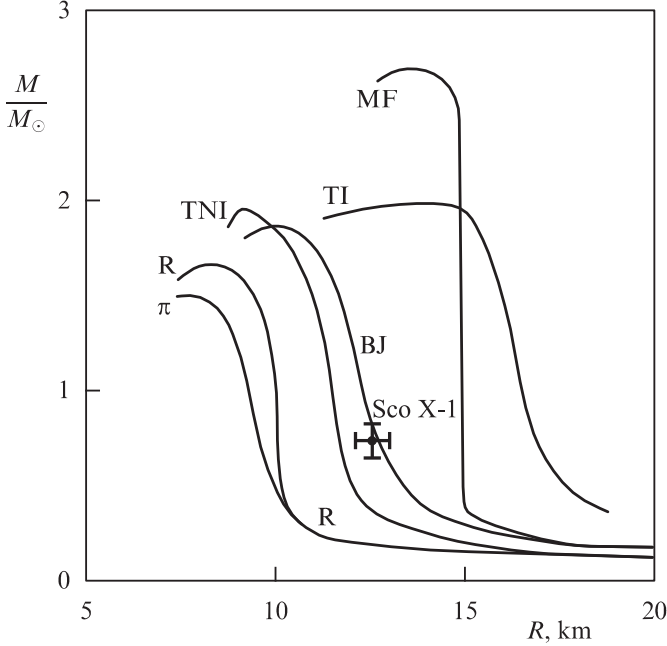
Fig. 8. Diagram of the dependence of gravitational mass on the radius for different equations of state of nuclear matter (Baym & Pethick 1979) and our point for Sco X-1 on it. Larger neutron star radii are given by stiff (TI, MF) rather than soft (R, π) equations of state. The classification corresponds to Alcock et al. (1986).

Méndez & van der Klis (1999) have observed that the separation between the two high-frequency QPO peaks changes from one observation to another. In our work we considered the equation

$$i \cdot (\omega_{\mathrm{K}} - \Omega) = \omega_j \simeq j \cdot \omega_{\mathrm{A}}. \tag{29}$$

In general case the peak separation will be

$$\omega_{\mathrm{K}} - \omega_{\mathrm{A}} = \frac{j}{i}\omega_{\mathrm{A}} + \Omega - \omega_{\mathrm{A}} = \left(\frac{j}{i} - 1\right)\omega_{\mathrm{A}} + \Omega. \tag{30}$$

It is easy to see, that when $i \neq j$ the peak separation will not remain constant. For example, if $i = 2$ and $j = 1$ then $\omega_{\mathrm{K}} - \omega_{\mathrm{A}} = -\omega_{\mathrm{A}}/2 + \Omega$. If $i = 1$ and $j = 2$, then $\omega_{\mathrm{K}} - \omega_{\mathrm{A}} = \omega_{\mathrm{A}} + \Omega$. Here we must mention that Alfven eigen frequency depends on the parameter λ that changes when f will change and, therefore, when f changes, numbers i and j can change. As a result, the dependence of the peak separation on ω_{K} will be a piece linear function. The dependencies of separation frequency on the lower one for different objects is shown on the Fig. 7. For Sco X-1 the dependence can be well approximated by the linear function (30) with $j/i = 3/4$ and $\Omega = 2\pi \cdot 450 \ \mathrm{s}^{-1}$.

So, comparing the 45 Hz QPO with Lense-Thirring precession we determine the ratio $M/R \approx 0.60$. Finally $M = 0.75 M_{\odot}$, $R = 12.6$ km, $T = 27$ eV. The point (M, R) on the gravitational mass – radius diagram is shown on the Fig. 8.

For this M, R, T we can find that $\omega_{0s} = 4.16 \ \mathrm{s}^{-1}$ or $\nu_{0s} = 0.66$ Hz. This low value can be explained by the
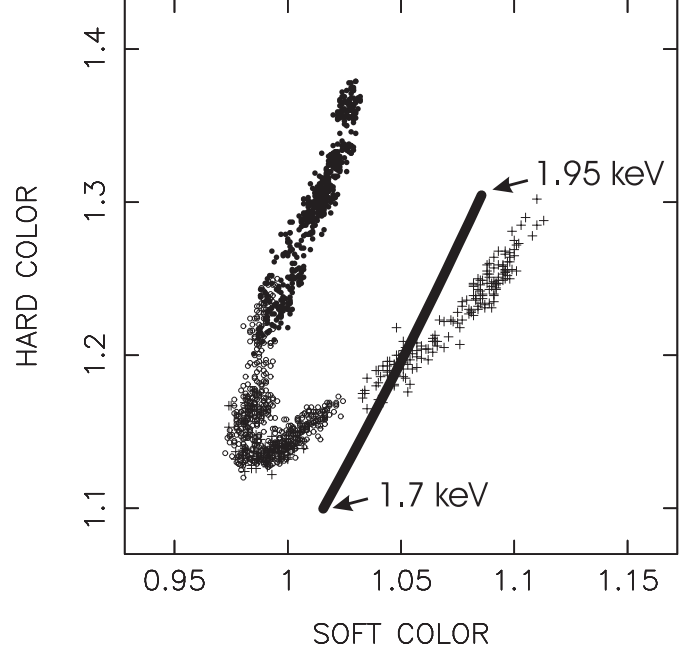

Fig. 9. The X-ray color-color diagram for Sco X-1 (van der Klis et al. 1996). Soft color is the (3-5 keV)/(1-3 keV), hard color the (7-20 keV)/(5-7 keV), count rate ratio. The bold line corresponds to the black body radiation with temperature varying from 1.7 keV to 1.95 keV.

fact that disk approaches too close to the neutron star (down to $f = 1.01$) and in this region of f function $\omega'_{\mathrm{s}}(f)$ takes values much greater than 1 (e.g. $\omega'_{\mathrm{s}}(1.01) = 15.7$).

At first sight, T must be equal to the radiation temperature of the neutron star, which can be determined from the X-ray color-color diagram. We put it on one graph from Scorpius X-1 and from black body (see Fig. 9). The normal branch of that from Scorpius almost coincide with that of black body. And the temperature of the black body varies from 1.7 keV up to 1.95 keV. But if we estimate the free path of the photons from the neutron star $\langle l \rangle \sim 1/\sigma n_{\mathrm{p}} \simeq 20$ km we find that it is greater then R and so, radiation does not heat the inner part of the disk.

References

Alcock, C., Farhi, E., & Olinto, A. 1986, ApJ, Vol. 310, 261

Baym, G. & Pethick, C. 1979, ARA&A, Vol. 17, 415

Klein, R. I., Jernigan, J. G., Arons, J., Morgan, E. H., & Zhang, W. 1998, ApJ, Vol. 508, 791–830

Méndez, M. & van der Klis, M. 1999, ApJ, Vol. 517, L51–54

Miller, M. C., Lamb, F. K., & Psaltias, D. 1998, ApJ, Vol. 508, 791–830

Morsink, S. M. & Stella, L. 1999, ApJ, Vol. 513, 827–44

Stella, L. & Vietri, M. 1999, Phys. Rev. Lett., Vol. 82, 17

Thorne, K. S., Price, R. H., & Macdonald, D. A. 1986, Black Holes: The Membrane Paradigm (Yale University Press)

Titarchuk, L. & Osherovich, V. 1999, ApJ, Vol. 518, L95–98

van der Klis, M. 2000, ARA&A, Vol. 38, 717–760

van der Klis, M., Swank, J. H., Zhang, W., Jahoda, K., & Morgan, E. H. 1996, ApJ, Vol. 469, L1–4